A low cost meteor observation system using radio forward scattering and the interferometry technique

Waleed Madkour, Masa-yuki Yamamoto, Yoshihiro Kakinami and Satoshi Mizumoto.

Electronic and Photonic Systems Engineering, Kochi University of Technology, Kami city, Kochi, Japan, 782-8502.

Corresponding author: W. Madkour, Electronic and Photonic Systems Engineering, Kochi University of Technology, Kami city, Kochi, Japan, 782-8502.

Email: 186006f@gs.kochi-tech.ac.jp ,

Tel: +818031607433, +81887572231

Abstract

We present a low cost meteor observation system based on the radio forward scattering and interferometry technique at Kochi University of Technology (KUT). The system can be a suitable model for low budget educational institutes that target practical learning of astronomical objects and upper atmospheric characteristics. The system methodology for the automatic counting of meteor echoes, filtering noise and detecting meteor echo directions is described. Detection of the meteor echo directions, which is the basic element for determining the meteor trajectories and the orbital parameters of parent comets, is based on a software system developed for analysis of phase differences detected by interferometry. Randomly selected observation samples measured by the radio interferometer are compared to simultaneous optical observations by video cameras to verify the system accuracy. Preliminary error analysis revealed that the system accuracy is directly related to the duration of observed meteor echoes. 80% of meteor echo samples with durations longer than 3 seconds showed agreement in azimuth and elevation angles measurements to within a 10 degree error range, while meteor echo samples with shorter durations showed lower agreement levels probably due to the low system sampling resolution of 0.1 seconds. The reasonable agreement level of meteor echoes with duration longer than 3 seconds demonstrated the applicability of the system methodology. Accurate observation of shorter duration meteor echoes could possibly be achieved by improving the system resolution.

Keywords:
Meteors; Radar; Forward scattering; Interferometry.

1. Introduction

The scattering of radio signals from ionized meteor trails provides a continuous method for meteors observations irrespective of weather conditions. The continuity advantage of this method over other optical methods enables persistent tracking of every meteor shower and guarantees capturing of irregular meteor showers that rarely bypass earth's atmosphere over decades or even centuries such as the Camelopardalids meteor shower in May 2014, originated from the newly discovered comet 209P/LINEAR. The Camelopardalids peaked for only few hours during which some locations on the Earth were unable to observe optically the new shower due to coincident bad weather, whereas the meteor radars across the globe were able to continuously observe the meteor shower parameters [e.g. Younger et al., 2015]. The observation capability of meteor radars is not limited to the detection and counting of meteors, but can also be extended to include the estimation of the orbital parameters of the parent comets of meteor showers [e.g., Janches et al., 2014, Younger et al., 2009; Webster et al., 2004]. From another aspect, meteor radars can be utilized for planetary science purposes by observing the physical and chemical interaction behavior upon the entry of meteoroids to the Earth's atmosphere such as the mesospheric ozone concentration [e.g., *Cevolani & Pupillo*, 2003], the mesospheric temperatures [e.g., *Hocking et al.,* 1997] and the upper atmospheric wind speeds [e.g., *Birkemeier et al*., 1973].

The orbits of parent comets are deduced by the analysis of the meteor showers parameters such as trajectory, velocity, and mass. A direction finding technique is necessary for the determination of these parameters. The phase difference detection by interferometry can be used for this. Interferometric meteor radar systems vary in size, power, technique and cost. High-power large-aperture (HPLA) radar systems with tens of arrayed antennas such as the monostatic Middle Atmosphere Alomar Radar System (MAARSY) in Norway or the Middle and Upper radar (MU radar) in Japan are normally constructed by high budget research institutes. These large scale systems use complex interferometric analysis over large number of receiving channels to detect the phase differences as, for example, the phase detection mechanism of the MAARSY system [Chau et al., 2014]. On the other hand, low budget educational institutes and amateur observer

groups cannot afford to build systems at this level and they tend to build alternative basic systems such as the one described in this paper.

The forward scattering observation system, although is geometrically more complex than the backscatter system, has the advantages of lower power requirements and longer duration meteor echoes. The presented receiver configuration follows the interferometry configuration explained by Jones et al. [1998]. This configuration could be familiar to the radio meteor observers worldwide, however, it remains a challenging task to construct a reliable algorithm to automate the continuous observation of the meteor showers parameters. The developed software structure is explained along with sample observational results of meteor echo directions compared to simultaneous video cameras observations to verify the effectiveness of the methodology.

2. System Description

The five channels KUT meteor observation system utilizes forward scattering of 53.75 MHz radio signals transmitted from the Sabae station, Fukui, Japan (Fukui National College of Technology: FNCT) at a distance of 340 km from Kochi (Figure 1). The system comprises of three subsystems; the transmitter, the receiver and the operating software.

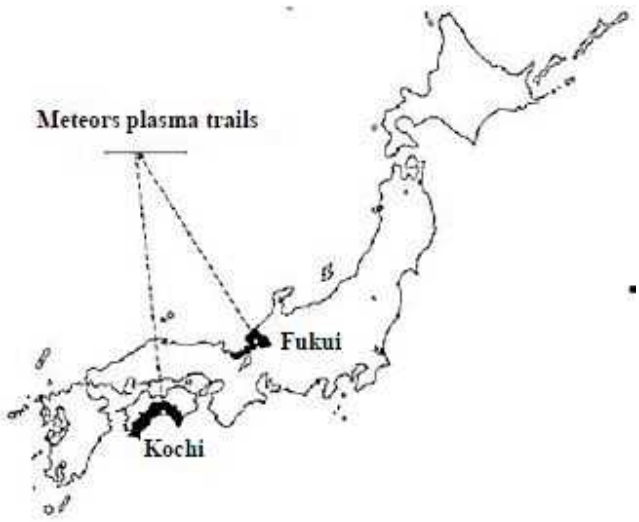

Fig.1 Transmitter location at Fukui (35°56'14.4" N, 136°10'18.9" E) and meteor radar location at Kochi University of Technology (33°37'16.5" N, 133°43'11.7" E).

2.1 Transmitter

Since 1999, a transmitter has been operated for radio meteor observation general use all over Japan. A two elements crossed Yagi antenna is used to transmit continuous wave (CW) at 50 W power and 53.75 MHz frequency from Sabae station generated by an ICOM IC-706 transmitter. The transmitter was designed to radiate an Omni-directional pattern over a wide range of elevation with more than 70^{o} zenith angle [Maegawa, 1999].

2.2 Receiver

Five crossed Yagi antennas in an elongated cross pattern setup with a common central antenna are used to receive radio signals scattered from meteor ionized trails (Figure 2). The antenna configuration was designed to apply the interferometry technique to incident waves in order to determine the precise direction of meteor echoes. The basic principle of interferometry is applied between any two independent antennas from the five to obtain phase differences. As shown in Figure 3, the wave path difference D between received signals is directly proportional to the spacing between the two antennas d by:

$$D = d.\sin\theta \ , \tag{1}$$

where θ is the angle of arrival of incoming waves.

The phase shift φ depends on the path difference D as well as on wavelength λ of the observing frequency by:

$$\varphi = (2\pi D)/\lambda \ , \tag{2}$$

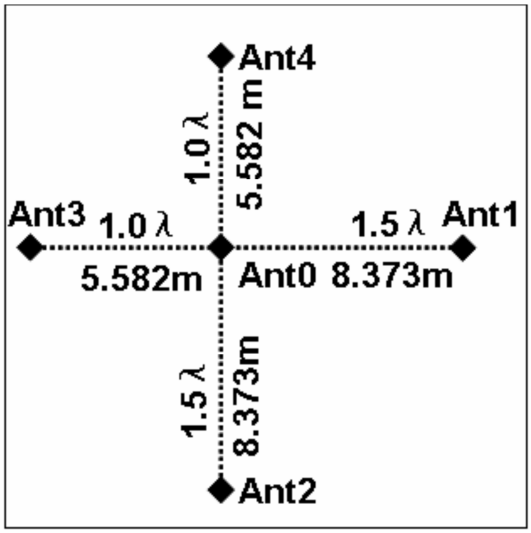

Fig.2 Antenna configuration of KUT interferometer.

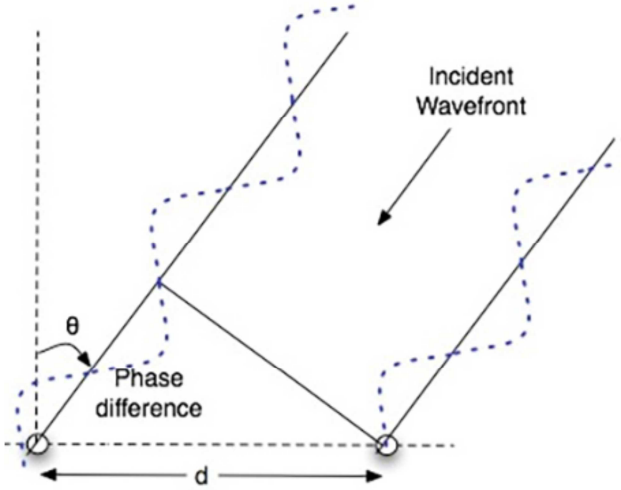

Fig.3 Interferometry principle.

To measure the angle of arrival accurately using the interferometer, the antenna spacing was selected as a compromise between the periodic ambiguity resulted from the use of a long spacing (multiples of 2π) and the mutual coupling resulting from the use of a short spacing (spacing less than or equal to 0.5λ). This can be optimally achieved by selecting adjacent antennas spacing meridionally or zonally so that the difference between them is equal to 0.5λ [*Jones et al*., 1998]. For the antennas configuration shown in Figure 2, two estimates of angle of arrival exist, the first is from the difference in spacing $\overline{Ant0Ant1} - \overline{Ant0Ant3} = 0.5\lambda$, which gives a low accuracy single estimation with no periodic ambiguity, while the second is from the total spacing

$\overline{Ant0Ant1} + \overline{Ant0Ant3} = 2.5\lambda$, which gives estimates with high accuracy but with periodic ambiguity. Figure 4 represents an example of phase estimation where the single estimation in the case of a short spacing removes the ambiguity present for the long spacing.

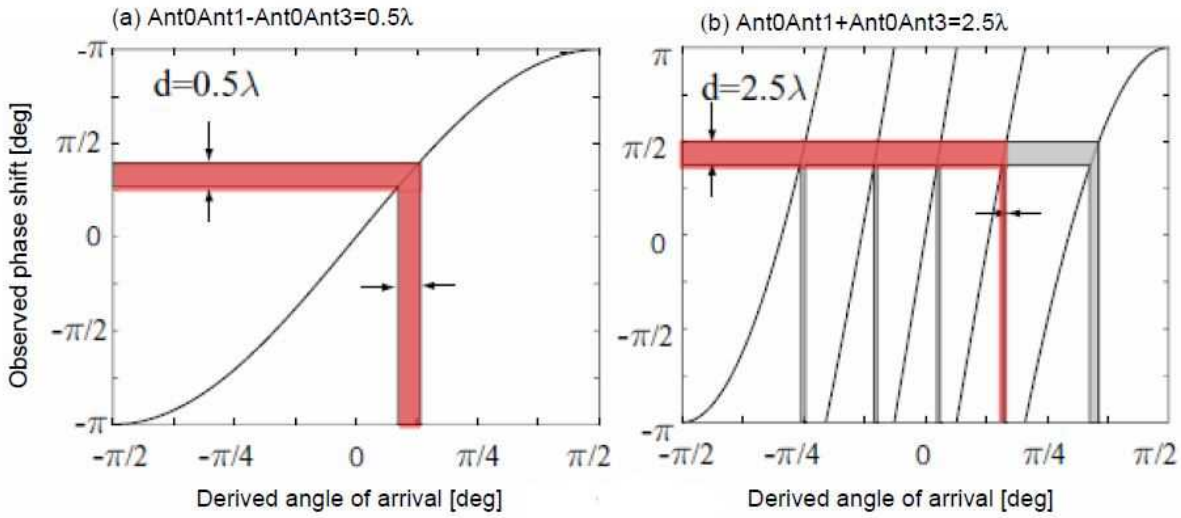

Fig.4 Relationship between observed phase shift and derived angle of arrival for cases of (a) difference in spacing: 0.5λ and (b) total spacing: 2.5λ (Figure 2). Shaded areas indicate the error range in phase observation and in the angle of arrival estimation.

The radio signals received by the five antennas are fed into a hardware system of five receivers, a PC with a multiple channel A/D board (SAYA, ADX85-1000), and a Garmin GPS circuit for accurate time synchronization (Figure 5). The receivers are of a super-heterodyne design, where the radio frequency detected is triple down-converted to a baseband signal. For our case using a received signal at 53.75 MHz, a 43.055 MHz oscillator for the first local signal and a 10.6941 MHz one for the second are selected. The 2 local signals are mixed with the received radio signal and BFO (beat frequency oscillator) of 455 kHz to produce a 900 Hz audio output signal. Interferometric information of each meteor echo is then realized by data analysis on the PC, where an A/D board of 1 MHz sampling in total with eight analog inputs is used for five channel data acquisition from the receivers, in addition to one channel for an accurate timing signal of one PPS (pulse per second) provided by the GPS receiver. From the common local oscillators, each

local signal is distributed to the five channels so as to maintain the observed phase shift into the down-converted signals.

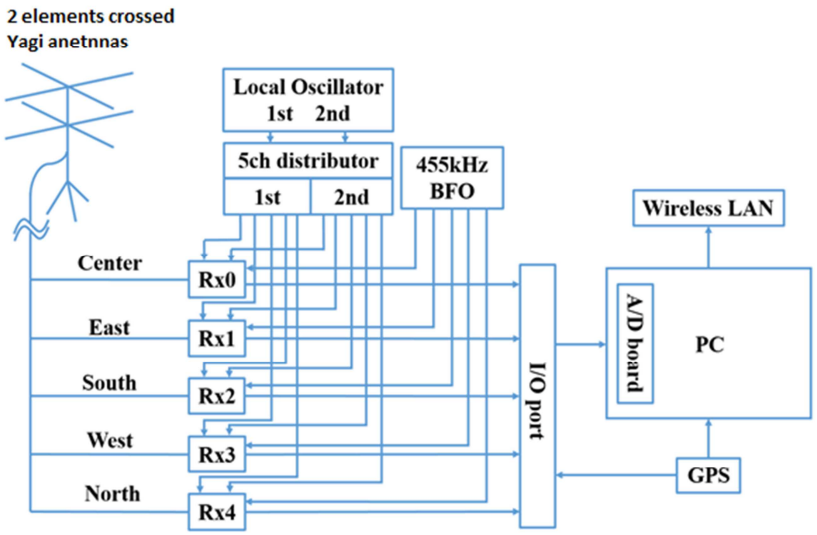

Fig.5 Block diagram of the 5 channel receiver.

2.3 Operating Software

A common software used in radio meteor observations in Japan, HROFFT (Ham-band Radio meteor Observation Fast Fourier Transform), generates spectrogram images for meteor echoes in 10 minute intervals with a total of 144 images per day. As the counting of meteor echoes on the spectrograms manually is not considered a standard method and consumes a lot of effort and time, a free software "Meteor echo counter" was developed at KUT in 2007 to automatically count meteors based on image processing techniques. It can also distinguish between meteor echoes and noise disturbances from other sources such as airplanes and thunderstorms [*Noguchi and Yamamoto*, 2008]. The software was then upgraded in 2008 to analyze the interferometeric phase differences and generate information on meteor echo directions every 10 minutes.

The operating software of the interferometer consists of three parts: (1) a sampling program for the A/D board interface to create a fixed-size swapping input file (7.5 seconds each) on a 128 MB memory drive on the PC, (2) a file combining program gathers the 7.5-s swapped files and combines them into a ten minute data file with precise referring to the 1 PPS signal for time adjustment, and (3) the data analysis software "HRO-IF-V2" which calculates the phase shift between the two antennas on each of the E-W and N-S axes to deduce the 3-dimensional echo direction from the equations:

$$Azimuth : \alpha = \tan^{-1}(\cos\theta_2 / \cos\theta_1) \ , \tag{3}$$

$$Elevation : \beta = \cos^{-1}(\cos\theta_2 / \cos\alpha) = \cos^{-1}(\cos\theta_1 / \sin\alpha) \, , \tag{4}$$

where θ_1 and θ_2 are the angles of arrival of the incoming waves for East axis and South axis planes, respectively (Figure 6).

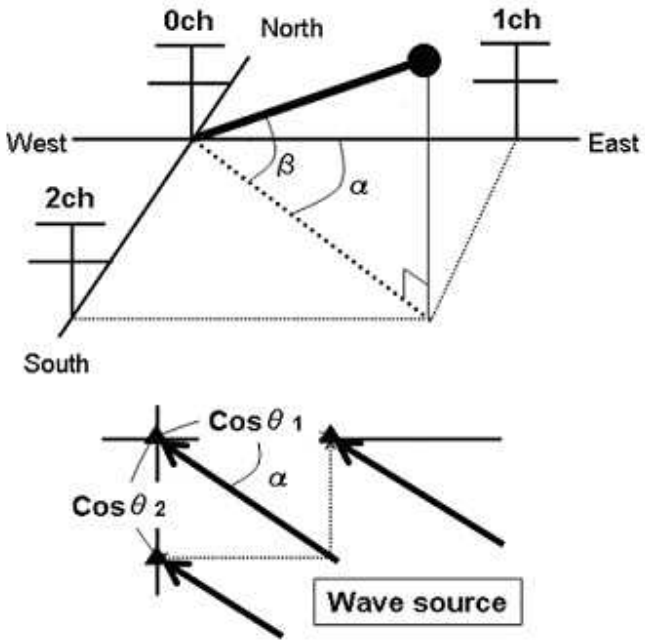

Fig.6 Azimuth and elevation angles determination by the interferometer (Unit vectors).

Phase spectrum analysis is performed by "HRO-IF-V2" to obtain the direction of each meteor echo, where a dynamic spectrum is created by FFT conversion into a frequency range of 850-1050 Hz every 0.1 second in addition to the detailed intensity profiles of the five independent channels with 43.4 kHz data sampling. The outcome of phase difference analysis can then be displayed by 'HRO-IF-VIEW' software that provides a graphical interface for the interferometric data. The 'HRO-IF-VIEW' output graph shown in Fig.7 consists of 5 vertical panels with a common horizontal time axis. The horizontal time axis is scaled in counts of 0.1 seconds for a maximum of 10 minute intervals (6000 counts). The meteor echo in Fig.7 was received during the 10 minutes interval from 3:00:00 to 3:10:00, between 100 and 250 counts after 3:00:00 (3:00:10 and 3:00:25). Vertically, The upper 2 panels display the elevation and azimuth angles, the middle panel displays the raw phase shifts between channel 0 and channel 1 (E-W axis) and between channel 0 and channel 2 (N-S axis), the real phase shift is plotted as cross marks by adding the calibration values, the fourth panel displays the relative signal amplitudes of channels 0, 1 and 2

used in phase difference determination, and lastly the bottom panel displays the amplitude dynamic spectrum in the range 850-1050 Hz divided in 20 steps, (e.g., in figure 7, the peak at 3 represents a frequency of 880 Hz).

3. Calibration

The correct output of phase shift analysis from interferometry by"HRO-IF-V2" is the most significant stage for the observation of meteor directions. In order to achieve a correct direction determination, calibration experiments by the interferometer in comparison with optical meteor observation were carried out. Video records of bright meteors taken at an adjacent location in KUT by a high-sensitivity CCD (Charge-Coupled Device) video cameras (Watec, Neptune-100N) with field of view (FOV) of 57° x 42° were used as absolute coordinate references.

A meteor image clearly captured by the video cameras on 4 January 2009 with azimuth and elevation angles of 349.4° and 43.9°, respectively, was used for calibration. As demonstrated in Figure 4, the phase differences corresponding to these values ought to provide two estimates for the 0.5λ and 2.5λ cases in each direction of E-W and N-S. Table 1 summarizes the calibration results that were used as a reference for interferometer observation including the intrinsic (instrumental) phase shift from the antennas to the receiver circuits. The estimated errors for phase uncertainty of ±5º are included.

Table 1. Calibration results derived from comparison with optical observation by video cameras.

	0.5λ		2.5λ	
	E-W	N-S	E-W	N-S
Calibration value	- 62.5°	+ 8.5°	- 272.3°	+ 12.8°
Estimated errors for phase uncertainty of ±5º	± 6.1º	± 6.1º	± 1.2º	± 1.2º

* Referring to Figure 4, for each direction, two phase estimates exist for each case of 0.5λ and 2.5λ. These calibration values were configured in the "HRO_IF_V2" software analysis to correct for intrinsic phase shifts.

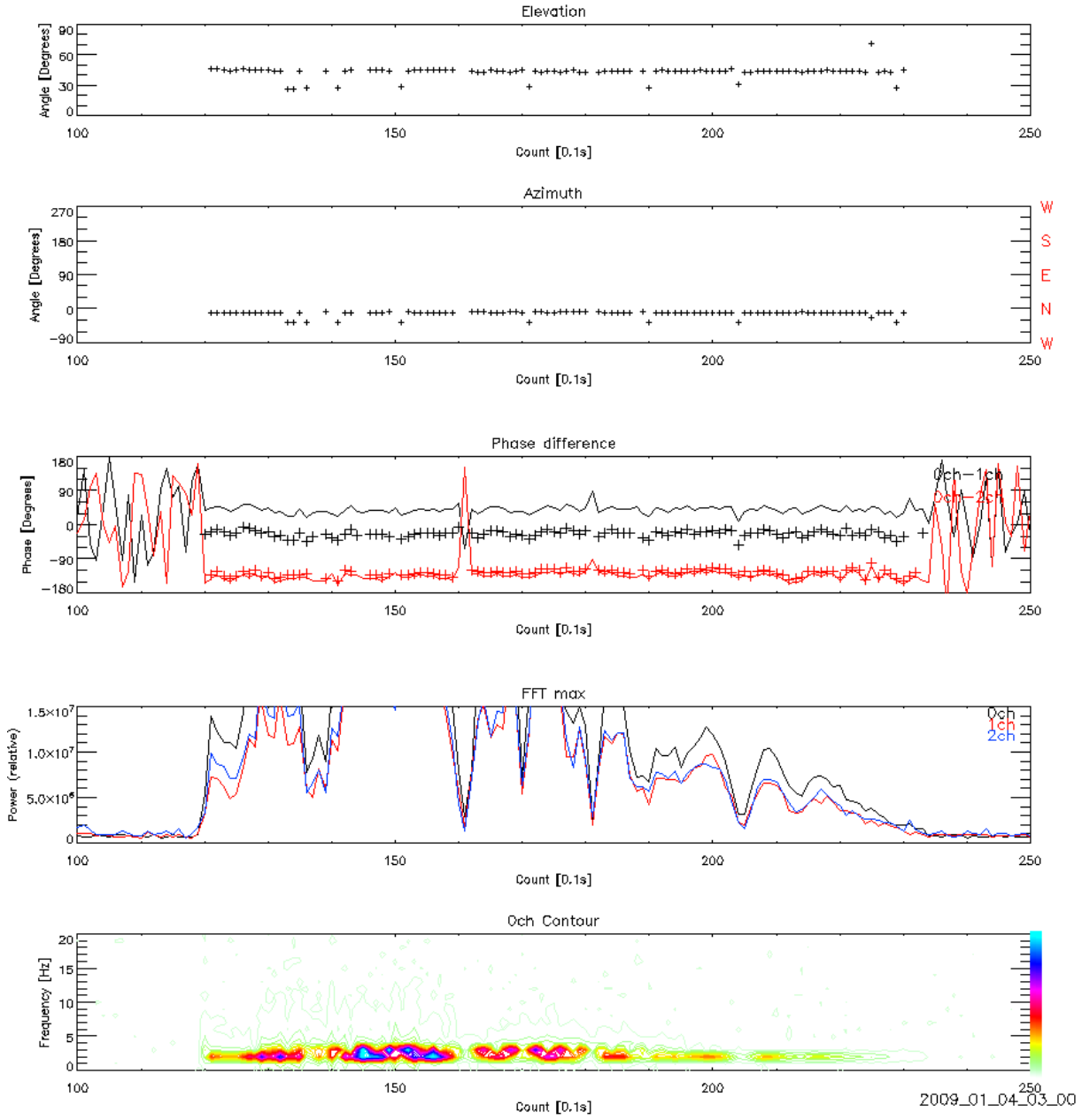

Fig.7 HRO_IF_VIEW graphical results for the interferometeric observation corresponding to the meteor trail image simultaneously captured by video cameras for calibration at 03:00:10 LT on 4 January 2009. The five vertical panels from up to down are: (a) Elevation angle, (b) Azimuth, (c) Phase difference for 0ch-1ch and 0ch-2ch, (d) Relative signal amplitudes of channels 0, 1, and 2, and (e) Dynamic spectrum of signal amplitude.

4. Selected Observational Results

The system efficiency in automatic counting of meteor echoes from HROFFT images using image processing was verified by Noguchi and Yamamoto [2008]. To test the accuracy of meteor echo direction measurements, selected simultaneous measurements by the interferometer and video cameras during and after the Quadrantid meteor shower (QUA) in 2009 are compared in Tables 2 and 3. Optical observation was performed using two video cameras in the north-west and south-east FOV at a location 40 meters away from the interferometer. The azimuth and elevation angles measurements were extracted from the text files generated from the interferometric analysis performed by "HRO_IF_V2" where the calibration values in Table 1 were preconfigured. Duration and intensity were measured by the "Meteor Echo Counter" software where the relative intensity is graded on 13 levels (from 0 to 12) according to the power spectrum of HROFFT spectrograms, where 0 is the lowest intensity level.

Among the all 42 results obtained in the selected period, there exist 20 records for meteor echoes with duration less than or equal to 3 seconds and 22 records for meteor echoes with duration longer than 3 seconds. The classification of meteor echoes into 2 categories according to their durations is due to the significant improvement observed in system accuracy for meteor echoes with durations more than 3 seconds. The system accuracy for different categories is discussed in the next section by error analysis.

Table 2. Simultaneous observation results by the interferometer (shaded rows) and video cameras (white rows) for the north-west direction (first camera FOV)

DATE YYYYMMDD	DETECTION TIME[LT]	AZIMUT ANGLE [DEG]	ELEVATION ANGLE [DEG]	DURATION [S]	INTENSITY [0-12] [A.U.]	
20090103	23:23:50	351	35	1	12	
	23:23:50	345	36			
20090104	01:29:33	338	38	10	12	
	01:29:33	346	42			
20090104	02:17:40	340	35	15	12	
	02:12:37	341	34			
20090104	03:00:11	350	44	12	12	
	03:00:10	349	44			
20090104	03:21:04	348	45	1	12	
	03:21:04	344	47			
20090104	03:27:46	350	37	11	12	
	03:27:44	350	39			
20090104	03:35:22	331	33	4	12	
	03:35:23	336	37			
20090104	03:36:21	341	34	10	12	
	03:36:21	340	35			
20090104	03:46:03	334	34	13	12	
	03:46:03	331	34			
20090104	04:30:22	356	64	4	12	
	04:30:22	352	64			
20090104	04:49:02	352	35	5	12	
	04:48:58	349	33			
20090104	04:58:11	166	51	1	8	
	04:58:10	359	23			
20090104	04:59:54	311	69	5	12	(3)
	04:59:50	330	45			
20090104	05:04:07	343	25	1	12	
	05:04:04	329	57			
20090104	05:16:44	308	57	11	12	(4)
	05:16:44	328	28			

20090104	05:23:22	68	14	1	9
	05:23:21	0	33		
20090104	05:29:57	176	51	1	10
	05:29:58	24	44		
20090127	05:57:21	301	54	8	10
	05:57:17	300	55		
20090127	21:13:22	307	50	4	12
	21:13:22	303	47		
20090128	00:50:58	248	75	1	9
	00:50:56	260	45		
20090128	04:15:06	311	50	5	10
	04:15:02	309	49		
20090128	04:44:33	304	63	5	12
	04:44:33	303	63		
20090129	04:29:46	330	38	2	12
	04:29:46	327	34		
20090201	03:39:48	302	52	8	12
	03:39:47	298	48		
20090202	00:55:03	290	33	1	12
	00:55:01	255	31		
20090203	03:57:48	286	33	11	12
	03:57:48	278	29		
20090212	02:34:29	295	52	16	12
	02:34:25	288	52		

Table 3. Simultaneous observation results by the interferometer (shaded rows) and video camera (white rows) for the south-east direction (second camera FOV).

DATE YYYYMMDD	DETECTION TIME [LT]	AZIMUTH ANGLE [DEG]	ELEVATION ANGLE [DEG]	DURATION [S]	INTENSITY [0-12] [A.U.]	
20090104	02:20:55	133	49	21	12	(1)
	02:20:54	100	65			
20090104	02:26:42	253	32	3	12	
	02:26:42	99	40			
20090104	03:04:49	142	17	1	8	
	03:04:44	145	69			
20090104	03:54:30	162	18	10	12	(2)
	03:54:30	160	54			
20090104	03:59:05	145	64	1	8	
	03:59:08	98	41			
20090104	04:01:41	119	50	3	12	
	04:01:41	158	70			
20090104	04:24:29	57	66	3	8	
	04:24:33	116	69			
20090104	05:13:26	317	79	3	12	
	05:13:26	160	50			
20090125	02:23:09	163	39	5	12	
	02:23:06	168	38			
20090128	22:11:39	134	55	3	9	
	22:11:36	130	57			
20090129	02:53:50	267	72	1	8	
	02:53:54	138	45			
20090202	04:25:15	313	61	1	9	
	04:25:18	161	54			
20090204	02:43:56	181	45	1	7	
	02:43:56	184	47			
20090204	03:20:57	25	51	1	6	
	03:20:57	159	26			
20090211	21:21:26	180	44	4	12	
	21:21:26	186	42			

5. Discussion

The observed duration and intensity of meteor echoes are included in Tables 2 and 3 to highlight their impact on the accuracy of interferometer direction determination. The error distribution results for the different categories are summarized in Fig.10. Error analysis of the interferometer azimuth and elevation angles samples in Tables 2 and 3 showed 55% agreement with optical observations within an error range of 10 degrees (Fig.8). By filtering the analysis to only echoes with the maximum intensity (level 12), the agreement level was raised to 68%. Although the intensity levels are only indicative of the relative signal strength, not the signal to noise ratio (S/N), the intensity related improvement can agree with results of similar studies if the noise level is checked on the background of HROFFT images. Meteor echoes longer than 3 seconds showed a higher agreement level of 82% within 10 degrees error and 80% for the same type of echoes but with the maximum intensity level of 12 (Fig.9). This significant improvement is logically due to the long echo durations relative to the system sampling resolution of 0.1 seconds in "HRO_IF_V2" analysis which does not provide enough sampling points for shorter duration meteor echoes. On the other hand, higher intensity levels did not show a remarkable impact on the accuracy for this type of echoes.

Three of the four cases in disagreement out of the 22 meteor echoes with durations more than 3 seconds (marked by (1), (3) and (4) at the right most column of Tables 2 and 3) showed inconsistent azimuth and elevation records in the "HRO_IF_VIEW" graphs (Fig.11). This inconsistency can possibly be due to the presence of high trees and buildings around the interferometer test site location in KUT that may cause extra signal reflections. The fourth case marked by (2) at the right most column of Table 3 shows agreement in azimuth measurements but different elevation measurements although consistent. The event occurred during the peak flux period of Quadrantids meteor shower (QUA) and could be a result of two different meteors detected by each of video cameras and the interferometer.

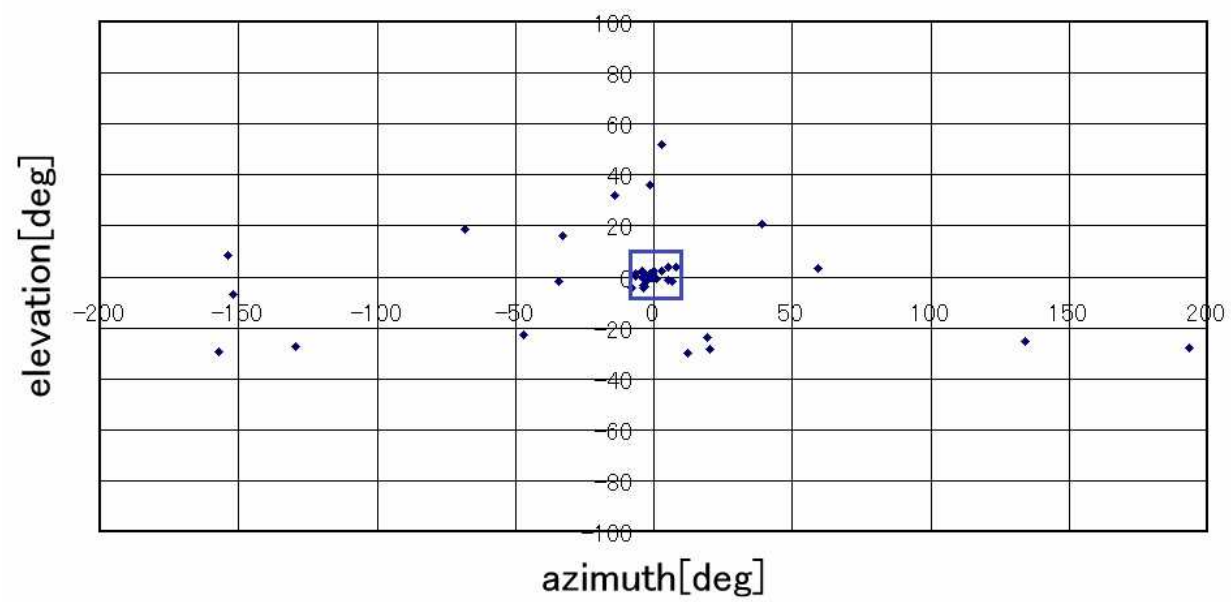

Fig.8 Error distribution for azimuth and elevation angles measurements in Table 3 and Table 4. The square represents 10 degrees error range.

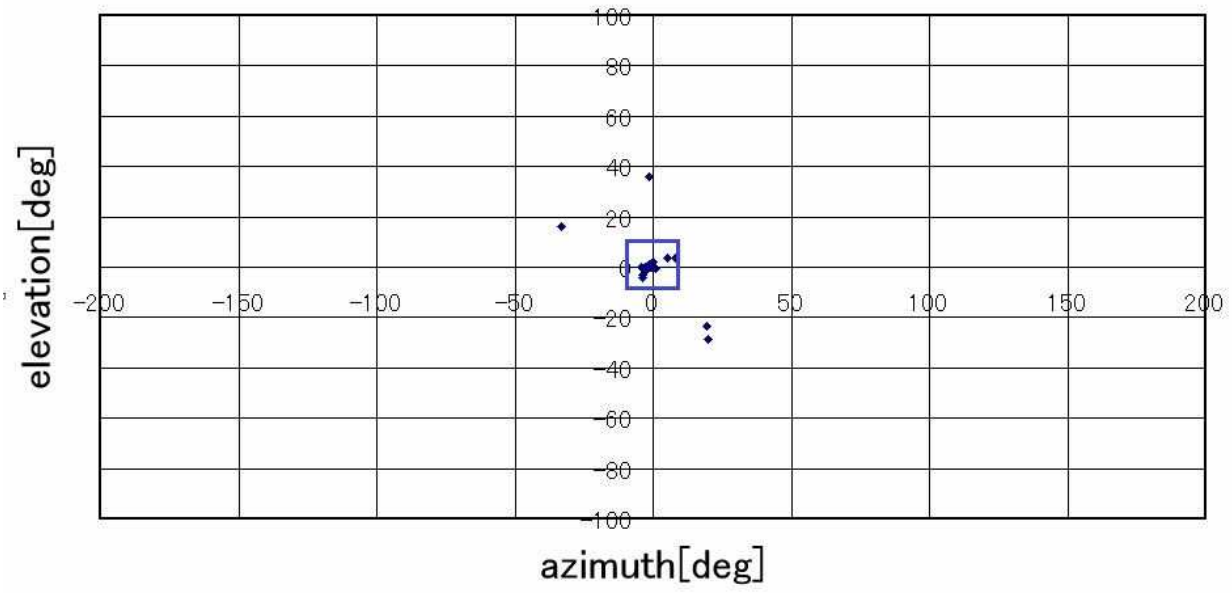

Fig.9 Error distribution for azimuth and elevation angles measurements for meteor echoes with duration more than 3 seconds and maximum intensity level (12).

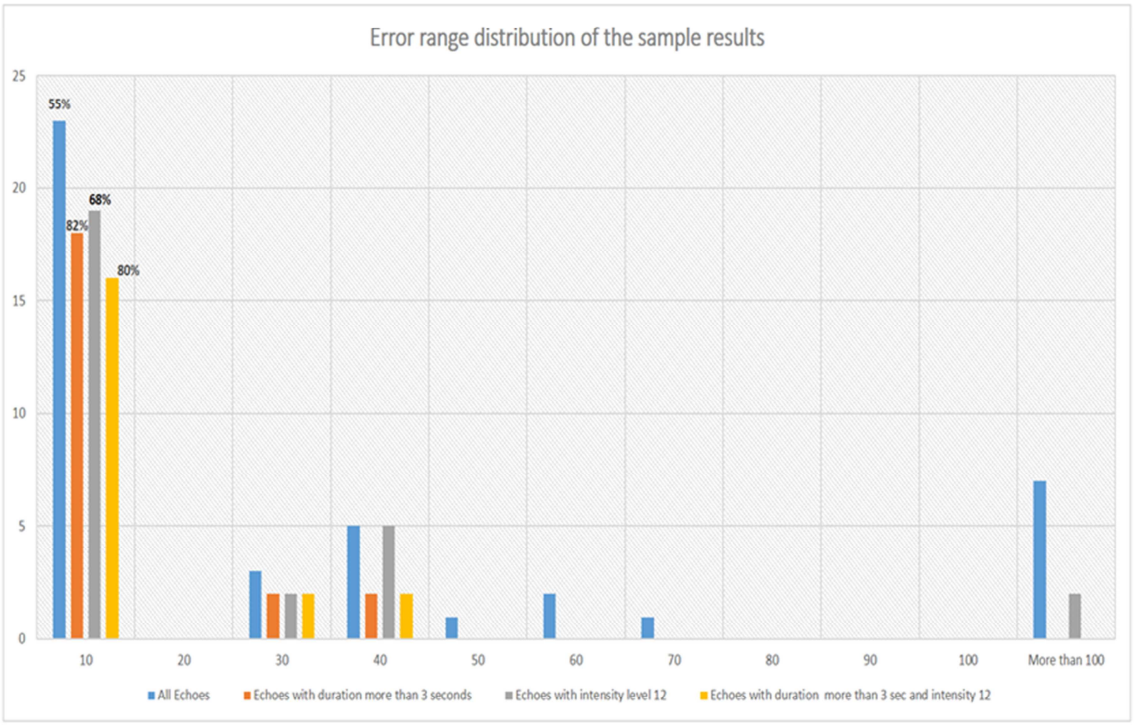

Fig.10 Error range distribution for the observational samples in Tables 2 and 3. The horizontal axis represents the error range in 10 degree steps for the maximum error among the azimuth or elevation angle measurements. The vertical axis represents the frequency of occurrence within the error ranges. The percentages are for the frequency of occurrence within 10 degrees error for each category.

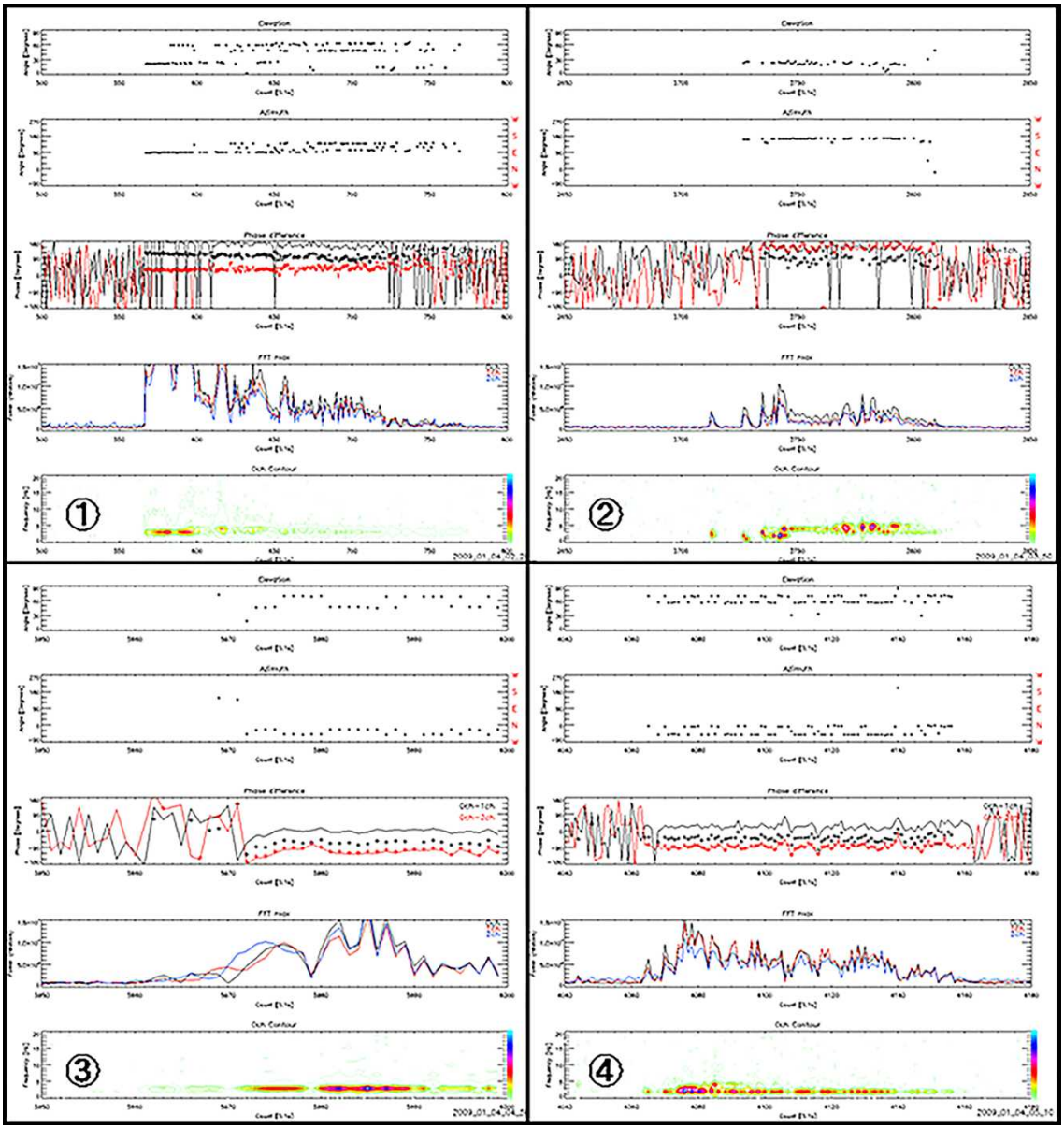

Fig.11 The same as in Fig.7 of "HRO_IF_VIEW" graphical output, but for the four mismatched cases with durations more than 3 seconds and maximum intensity level of 12. For the top two panels of azimuth and elevation angles, the plotted data show inconsistent scattered characteristics for cases of (1), (3) and (4). For case (2), azimuth and elevation measurements are consistent but the determined elevation was different from the optical observation.

6. Conclusion

A low cost methodology for meteor observations using radio forward scattering and the interferometry technique is presented. The developed system uses an image processing algorithm to filter several types of noise echoes and automatically count the number of meteor echoes in real time. It can also analyze the phase difference between 5 channels of received signals and generate text and graphical information about meteor echo directions. A period with simultaneous optical and radio observations was selected to verify the effectiveness of the system methodology and display its capabilities. Although the amount of the selected data remains insufficient to evaluate the constant performance of the system, it gives an indication about the system sensitivity to different types of meteor echoes. The average agreement level of 80% among the selected long duration observation samples (more than 3 s) reflects the system increasing efficiency in observing the direction of meteor echoes of this type. However, the existence of disagreement for some meteor echoes with long durations requires additional statistical analysis over larger amounts of simultaneous radio and optical observational data to decide the precise effect of surrounding obstacles (buildings and trees) on the interferometer measurements.

The automated measurement of meteor echo directions is considered the fundamental starting point towards a comprehensive study of meteor origins. Considering the low budget environment, a network of remote single-antenna detectors can gradually be established to provide accurate observation of meteor trajectories and velocities. At the present time, two additional receiving remote stations with single antenna each were established at distances of 23 and 13 kilometres away from the main KUT interferometer location. Future work could focus on developing an accurate automated observation algorithm using the multiple stations that allows the determination of each meteor trajectory and velocity. By observing the trajectory and velocity of each meteor, it might then be possible to not only deduce the orbital parameters of parent comets of meteor streams, but also to statistically study sporadic meteors behavior and deduce other possible origins of meteoroids such as the interstellar meteoroids [e.g. Weryk and Brown, 2005].

The system described in this paper has been developed by students at KUT with a low cost of around 6 thousand dollars excluding the transmitter cost at Sabae station. As the ham band common transmitter in Japan can be a special case, building a transmitting point with the same

specifications would add around one thousand dollars to the total cost in addition to the running cost of continuous power transmission. The developed software applications and source code are made free for interested observers worldwide to use or to develop any additional enhancements. There is scarcity of meteor observation records from several locations on Earth such as Africa and Middle East sector longitudinally or south America latitudinally. The authors aim that this paper may encourage low-budget educational and scientific institutes at these locations to build similar systems.

7. References

Birkemeier, W. P., A. B. Fontaine, K. S. Gage, S. A. Gronemeyer, W. H. Jasperson, and F.S. Sechrist, (1973), Wind Measurements Using Forward-Scatter CW Radar, *J. Appl. Meteor.*, 12, 1044–1053.

Cevolani, G and G. Pupillo (2003), Ground-based radio observations to probe the ozone content in the meteor region, *Annals of Geophysics*, 46, 247-258.

Chau, J.L., T. Renkwitz, G. Stober, and R. Latteck (2014), MAARSY multiple receiver phase calibration using radio sources, *Journal of Atmospheric and Solar-Terrestrial Physics,* 118, 55-63.

Hocking, W. K., T. Thayaparan, and J. Jones (1997), Meteor decay times and their use in determining a diagnostic mesospheric temperature-pressure parameter: methodology and one year of data, *Geophysical Research Letters,* Vol. 24, 23, 2977-2980.

Janches, D., W. Hocking, S.Pifko, J.L. Hormaechea, D.C. Fritts, C. Brunini, R. Michell, and M. Samara, (2014), Interferometric meteor head echo observations using the Southern Argentina Agile Meteor Radar, *Journal of Geophysical Research, Space physics,* Vol. 119, 3, 2269 – 2287.

Jones, J., A. R. Webster and W.K. Hocking, (1998), An improved interferometer design for use with meteor radars, *Radio Science*, 33, 55-65.

Maegawa. K (1999), HRO: a new forward-scatter observation method using ham-band beacon. *WGN* 27, 64-72.

Noguchi, K. and M-Y. Yamamoto (2008), Development of an automatic echo-counting program for HROFFT spectrogram, *Earth, Moon and Planets,* 102*,* 323-329.

Webster, A. R., P. G. Brown, J. Jones, K. J. Ellis, and M. Campell-Brown (2004), Canadian Meteor Orbit Radar (CMOR), *Atmos. Chem. Phys*., 4, 679–684.

Weryk, R.J. and P. Brown (2005), A search for interstellar meteoroids using the Canadian meteor orbit radar (CMOR), *Earth, Moon and Planets*, 95, 221-227.

Younger, J.P., I.M. Reid, R. A. Vincent, D. A. Holdsworth and D. J. Murphy, (2009), A southern hemisphere survey of meteor shower radiants and associated stream orbits using single station radar observations, *Mon. Not. R. Astron. Soc.* 398, 350–356.

Younger, J.P., I.M. Reid, G. Li, B. Ning, and L. Hu (2015), Observations of the new Camelopardalids meteor shower using a 38.9 MHz radar at Mohe, China, *Icarus,* 253, 25-30.

Acknowledgments

The source of data shown in this paper can be made available upon request from the author.

The authors thank Kazuya Noguchi for his valuable contribution to this work. They are also grateful for Kimio Maegawa for the long-term operation of continuous beacon transmission from Sabae station.

Figures Caption

Fig.1 Transmitter location at Fukui (35°56'14.4" N, 136°10'18.9" E) and meteor radar location at Kochi University of Technology (33°37'16.5" N, 133°43'11.7" E).

Fig.2 Antenna configuration of KUT interferometer.

Fig.3 Interferometry principle.

Fig.4 Relationship between observed phase shift and derived angle of arrival for cases of (a) difference in spacing: 0.5λ and (b) total spacing: 2.5λ (Figure 2). Shaded areas indicate the error range in phase observation and in the angle of arrival estimation.

Fig.5 Block diagram of the 5 channel receiver.

Fig.6 Azimuth and elevation angles determination by the interferometer (Unit vectors).

Fig.7 HRO_IF_VIEW graphical results for the interferometeric observation corresponding to the meteor trail image simultaneously captured by video cameras for calibration at 03:00:10 LT on 4 January 2009. The five vertical panels from up to down are: (a) Elevation angle, (b) Azimuth, (c) Phase difference for 0ch-1ch and 0ch-2ch, (d) Relative signal amplitudes of channels 0, 1, and 2, and (e) Dynamic spectrum of signal amplitude.

Fig.8 Error distribution for azimuth and elevation angles measurements in Table 3 and Table 4. The square represents 10 degrees error range.

Fig.9 Error distribution for azimuth and elevation angles measurements for meteor echoes with duration more than 3 seconds and maximum intensity level (12).

Fig.10 Error range distribution for the observational samples in Tables 2 and 3. The horizontal axis represents the error range in 10 degrees steps for the maximum error among the azimuth or elevation angles measurements. The vertical axis represents the frequency of occurrence within the error ranges. The percentages are for the frequency of occurrence within 10 degrees error for each category.

Fig.11 The same as in Fig.7 of "HRO_IF_VIEW" graphical output, but for the four mismatched cases with durations more than 3 seconds and maximum intensity level of 12. For the top two panels of azimuth and elevation angles, the plotted data show inconsistent scattered characteristics for cases of (1), (3) and (4). For case (2), azimuth and elevation measurements are consistent but the determined elevation was different from the optical observation.